Richa Sharma[1], Sanjeev Sharma[2], Zoran Radaković[5]

THERMAL CREEP ANALYSIS OF PRESSURIZED THICK-WALLED CYLINDRICAL VESSELS
TERMIČKA ANALIZA PUZANJA CILINDRIČNIH DEBELOZIDIH POSUDA POD PRITISKOM

Originalni naučni rad / Original scientific paper
UDK /UDC: 620.179.13:62-988
Rad primljen / Paper received: 16.08.2017

Adresa autora / Author's address:
[1)] Department of Mathematics, SBSR, Sharda University, Greater Noida, India email: richa.sharma@sharda.ac.in
[2)] Department of Mathematics, Jaypee Institute of Information Technology, Noida, India
[3)] University of Belgrade, Faculty of Mechanical Engineering, Belgrade, Serbia

Keywords
- creep
- cylinder
- internal pressure
- external pressure
- homogeneous
- thermal analysis

Ključne reči
- puzanje
- cilindar
- unutrašnji pritisak
- spoljašnji pritisak
- homogenost
- termička analiza

Abstract

Thermal stresses are calculated in thick-walled circular cylinder under internal and external pressure. The concept of transition theory and generalized strain measures is employed for the creep analysis of thick-walled cylinder. The mathematical modelling details of the methodology applied in this analysis are discussed extensively. Analytical method of solution has been applied to simplify the governing differential equations. The obtained results are presented in terms of graphs. On the basis of analysis, it has been deduced that less compressible thick-walled circular cylinder with thermal effects under the influence of internal and external pressure with non-linear measure is a better alternative for design engineers as compared to other cylinders.

Izvod

Termičko naponsko stanje je proračunato kod debelozide cilindrične posude pod uticajem unutrašnjeg i spoljnog pritiska. Koncept teorije prelaznih napona i generalisane mere deformacije su primenjeni za analizu puzanja debelozidog cilindra. Detalji matematičkog modeliranja primenjene metodologije u ovoj analizi su opisani i diskutovani. Analitička metoda rešenja je primenjena radi pojednostavljenja osnovnih diferencijalnih jednačina. Dobijeni rezultati su predstavljeni dijagramima. Na osnovu analize, izveden je zaključak da je slučaj modela termički opterećenog kružnog debelozidog cilindra manje stišljivosti pod dejstvom unutrašnjeg i spoljnog pritiska sa nelinearnom merom deformacija bolje rešenje za projektante u poređenju sa drugim modelima cilindra.

INTRODUCTION

Creep is an important phenomenon in the design analysis of cylinders. Creep is time-dependent deformation under constant load and temperature. In creep, a structural component undergoes time dependent change in stress and strain such as progressive deformation, relaxation and redistribution of stresses, reduction of material strength, changes of material behaviour from isotropic to anisotropic etc. Many authors such as Altenbach and Skrzypek /1/, Kraus /2/, have discussed on the creep deformation in thick-walled cylinders under internal pressure. Rimrott and Luke /3/ obtained creep stresses of a rotating hollow circular cylinder made of isotropic and homogenous material. Assuming the plane strain condition, Bhatnagar et al. /4/, analysed creep stresses in a pressurized, homogenous, rotating cylinder made of orthotropic material. Stress analysis in a homogeneous pressure vessel, having material creep behaviour is carried out by Kashkoli and Nejad /5/ by applying classical theory and it is concluded that all three stresses decrease with time. Loghman et al. /6/ studied creep stresses in hollow circular rotating cylinders made of exponentially graded material and concluded that creep strains and stresses have lower values in the rotating cylinder of functionally graded material. You et al. /7/ discussed steady-state creep of thick-walled cylindrical vessels made of functionally graded materials subjected to internal pressure in order to identify how stresses are affected by varying material parameters along the radial direction. Singh and Gupta /8/ carried out creep analysis in transversely isotropic functionally graded cylinder, operating under pressures and found that the magnitude of stresses and strain rates can be reduced by subjecting it to both internal and external pressures, though the stress non-homogeneity in the cylinder decreases. To find creep stresses and strains, the above-mentioned authors used the methodology of classical theory based on assumptions as incompressibility, infinitesimal strain theory and yielding criterions, etc. In fact, in most of the cases, it is not possible to find a solution in closed form without these assumptions. The transition theory /9/ does not require any of the above-mentioned assumptions of classical theory and thus it simplifies the problems more precisely by applying the generalized measure concept, /10/. This theory has been employed by various authors /11-17/, for example, Sharma /11/ evaluated thermal creep stresses in rotating cylinders

made of non-homogeneous material and it is found that a cylinder of less compressible material at the internal surface, and highly compressible at the outer surface is on the safer side. Sharma et al. /12/ studied the elastic-plastic stresses in transversely isotropic rotating cylinders under internal pressure and it is found that thick-walled cylinder of transversely isotropic material is safer for designing as compared to the isotropic cylinder. Aggarwal et al. /13/ investigated thermal stresses in thick circular cylinder of functionally graded material under internal and external pressure and it is found that compressible cylinder of functionally graded material is better than cylinders with other factors. Sharma /20/ determined thermal elastic-plastic stresses in thick-walled circular cylinder subjected to external loading while Sharma /21/ investigated creep stresses in bending of functionally graded plate to cylinder using Seth's transition theory with generalized strain measure.

In the presented work, our main aim is to analyse creep stresses and strain rates in thick homogeneous cylindrical pressure vessels with temperature without using the assumptions made in the classical theory of yielding, Norton's law, etc. Analytic method of computation is used to evaluate the stresses. Results are discussed numerically and presented graphically.

MATHEMATICAL MODELLING

Thick circular cylinder of radii 'a' and 'b' where ($a < b$), under pressures p_1 (at the inner surface) and p_2 (at the outer surface) with steady state temperature applied at the inner surface is taken into consideration.

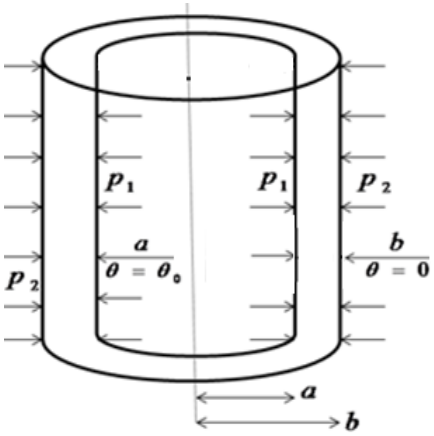

Figure 1. Geometrical representation of the problem.

The components of displacement in polar coordinates are given as

$$u_1 = r(1-\kappa),\ \ u_2 = 0,\ \ u_3 = \phi z \tag{1}$$

where: κ is a function of $r = \sqrt{x^2 + y^2}$; and ϕ is a constant. The generalized strain components /11/ are

$$\varepsilon_{rr} = \frac{1}{n}[1-(r\kappa' + \kappa)^n],\ \ \varepsilon_{\theta\theta} = \frac{1}{n}[1-\kappa^n],$$
$$\varepsilon_{zz} = \frac{1}{n}[1-(1-\phi)^n],\ \ \varepsilon_{r\theta} = \varepsilon_{\theta z} = \varepsilon_{rz} = 0\,. \tag{2}$$

The Hooke's law for isotropic material is,

$$\tau_{rr} = \lambda I_1 + \frac{2\mu}{n}\left\{1-(r\kappa' + \kappa)^n\right\} - \xi T\,,$$
$$\tau_{\theta\theta} = \lambda I_1 + \frac{2\mu}{n}\left\{1-\kappa^n\right\} - \xi T\,,$$
$$\tau_{zz} = \lambda I_1 + \frac{2\mu}{n}\left\{1-(1-\phi)^n\right\} - \xi T\,,$$
$$\tau_{zr} = \tau_{\theta z} = \tau_{r\theta} = 0\,, \tag{3}$$

where: $I_1 = \frac{1}{n}\left[3-(r\kappa' + \kappa)^n - \kappa^n - (1-\phi)^n\right]$.

Equations (3) can also be written as

$$\tau_{rr} = \left(\frac{\lambda+2\mu}{n}\right)\left(1-(r\kappa' + \kappa)^n\right) + \frac{\lambda}{n}(1-\kappa^n) + \lambda k - \xi T\,,$$
$$\tau_{\theta\theta} = \left(\frac{\lambda}{n}\right)\left(1-(r\kappa' + \kappa)^n\right) + \left(\frac{\lambda+2\mu}{n}\right)(1-\kappa^n) + \lambda k - \xi T\,,$$
$$\tau_{zz} = \left(\frac{\lambda}{n}\right)\left(1-(r\kappa' + \kappa)^n\right) + \left(\frac{\lambda}{n}\right)(1-\kappa^n) + (\lambda+2\mu)k - \xi T\,,$$
$$\tau_{zr} = \tau_{\theta z} = \tau_{r\theta} = 0\,. \tag{4}$$

where: $k = \frac{1}{n}\left(1-(1-\phi)^n\right)$, and $\xi = \alpha(3\lambda + 2\mu)$.

The equation of cylinder in equilibrium state is

$$\frac{d}{dr}(\tau_{rr}) + \left(\frac{\tau_{rr} - \tau_{\theta\theta}}{r}\right) = 0\,. \tag{5}$$

The temperature is given by

$$T = \frac{T_0}{\mathrm{Log}(a/b)}\mathrm{Log}(r/b)\,, \tag{6}$$

where: T_0 is a constant.

The governing differential equation of the problem is obtained from Eqs.(4) and (5) as

$$\kappa\eta(1+\eta)^{n-1}\frac{d\eta}{d\kappa} + \left(\eta + \frac{C}{n}\right)(1+\eta)^n + \eta(1-C) - \frac{C}{n} + \frac{C\xi\overline{T}_0}{2\mu\kappa^n} = 0\,, \tag{7}$$

where: $r\kappa' = \kappa\eta$.

The transitional point in the above equation is $\eta \to -1$.

The pressure at the boundaries of the cylinder is taken as

$$\tau_{rr} = -p_1 \ \text{ at } \ r = a\,;\ \ \tau_{rr} = -p_2 \ \text{ at } \ r = b. \tag{8}$$

The resultant axial force is given by

$$2\pi\int_a^b r\,\tau_{zz}\,dr = 0\,. \tag{9}$$

SOLUTION THROUGH TRANSITION FUNCTION

In classical theory, authors /1-8/ considered the assumption of infinitesimal strain theory, Norton's law, etc. The authors in /9-17/ use the concept of transition theory to find the creep stresses. In this paper, we also consider the concept of transition theory which eliminates the use of jump conditions of classical theory. Here, we consider a transition function *TR* which is considered as stress difference. This type of transition function is considered only because of the reason that transition from elastic to creep region is going through the principal stresses. Hence we can consider either the principal stresses as transition function

or difference of principal stresses as transition function. The transition function *TR* is defined as

$$TR = \tau_{rr} - \tau_{\theta\theta} = \frac{2\mu\kappa^n}{n}\left[1-(\eta+1)^n\right] \tag{10}$$

Taking logarithmic differentiation of Eq.(10) with respect to *r*, we get

$$\frac{d}{dr}(\mathrm{Log}\,TR) = \frac{n\eta}{r} - \frac{n\eta\kappa(\eta+1)^{n-1}\dfrac{d\eta}{d\kappa}}{r\left[1-(\eta+1)^n\right]}. \tag{11}$$

By substituting the value of $d\eta/d\kappa$ from Eq.(7) into Eq.(10) and taking asymptotic value of κ as $\eta \to -1$, we get

$$\frac{d}{dr}(\mathrm{Log}\,TR) = -\frac{2n}{r} + \frac{(n-1)C}{r} + \frac{nC\xi\overline{T_0}}{2\mu r\kappa^n}. \tag{12}$$

Integrating Eq.(12), we get

$$TR = A'\frac{1}{r^{2n-nC+C}}\exp f\,, \tag{13}$$

where: $f = \int\left(\dfrac{nC\xi\overline{T_0}}{2\mu r\kappa^n}\right)dr$, and A' is integration constant.

By using Eqs.(13) and (10), it is found that

$$\tau_{rr} - \tau_{\theta\theta} = A'rG\,, \tag{14}$$

where: $G = \dfrac{1}{r^{2n+1-nC+C}}\exp f$.

By using Eqs.(5) and (14), the following results are obtained:

$$\tau_{rr} = B' - A'\int G dr\,, \tag{15}$$

where: B' is integration constant.

Values of constants *A* and *B*, obtained by Eq.(8) are

$$A' = \frac{p_1 - p_2}{\int_a^b G dr}\,; \quad B' = -p_2 + \frac{p_1 - p_2}{\int_a^b G dr}\left[\int G dr\right]_{r=b}.$$

From Eq.(15), we have the thermal radial creep stress as

$$\tau_{rr} = -p_2 + A'\int_r^b G dr\,. \tag{16}$$

Using Eqs.(5) and (16), we have thermal circumferential creep stress as

$$\tau_{\theta\theta} = -p_2 + A'\left[\int_r^b G dr - rG\right]. \tag{17}$$

Using Eq.(4), Eqs.(15) and (16), we obtain the thermal axial creep stress as

$$\tau_{zz} = \left(\frac{1-C}{2-C}\right)(\tau_{rr}+\tau_{\theta\theta}) + 2\mu\left(\frac{3-2C}{2-C}\right)\varepsilon_{zz} - 2\mu\left(\frac{3-2C}{2-C}\right)\alpha T\,, \tag{18}$$

where:

$$\varepsilon_{zz} = \frac{-\int_a^b \dfrac{r(1-C)}{(2-C)}\left[\tau_{rr}+\tau_{\theta\theta}\right]dr + \mu\alpha T(b^2-a^2)\left(\dfrac{3-2C}{2-C}\right)}{\mu\left(\dfrac{3-2C}{2-C}\right)(b^2-a^2)}.$$

Equations (16)-(18) give creep stresses with temperature. Components in non-dimensional form are taken as follows:

$R_0 = \dfrac{a}{b}$; $R = \dfrac{r}{b}$; $\sigma_r = \dfrac{\tau_{rr}}{\gamma}$; $\sigma_\theta = \dfrac{\tau_{\theta\theta}}{\gamma}$; $\sigma_z = \dfrac{\tau_{zz}}{\gamma}$; $\dfrac{\alpha T_0}{\gamma} = T_1$;

$\dfrac{p_1}{\gamma} = P_1$; $\dfrac{p_2}{\gamma} = P_2$; $\dfrac{p_1 - p_2}{\gamma} = \dfrac{p}{\gamma} = P$; $\varepsilon^*_{zz} = \dfrac{\varepsilon_{zz}}{\gamma}$; and γ is Young's modulus.

The following equations are obtained by converting Eqs.(16)-(18) in non-dimensional form

$$\sigma_r = -P_2 + A_1\int_R^1 G^* dR\,, \tag{19}$$

$$\sigma_\theta = -P_2 + A_1\left[\int_R^1 G^* dR - bRG^*\right], \tag{20}$$

$$\sigma_z = \left(\frac{1-C}{2-C}\right)(\sigma_r+\sigma_\theta) + \varepsilon^*_{zz} - T_1\frac{\log R}{\log R_0}\,, \tag{21}$$

where: $A_1 = \dfrac{P}{\int_{R_0}^1 bG^* dR}$; $G^* = \dfrac{1}{(bR)^{2n+1-nC+C}}\exp f^*$;

$$f^* = \int\frac{nT_1(3-2C)}{\kappa^n R\log R_0}dR\,;$$

$$\varepsilon^*_{zz} = \frac{-\int_{R_0}^1 b^2R\left(\dfrac{1-C}{2-C}\right)(\sigma_\theta+\sigma_r)dR + \dfrac{T_1(\log R/\log R_0)}{2}(1-R_0^2)}{\dfrac{1}{2}(1-R_0^2)}.$$

STRAIN RATES

The Hooke's law in terms of strain rates can be written as

$$\dot{\varepsilon}_{ij} = \frac{(1+\nu)}{\gamma}\sigma_{ij} - \frac{\nu}{\gamma}\delta_{ij}\Theta + \alpha T\,, \tag{22}$$

where: $\dot{\varepsilon}_{ij}$ is the strain rate tensor; and $\Theta = \sigma_{ij}$; ($i = j$) and $\nu = \dfrac{1-C}{2-C}$.

The following equation is obtained by differentiating Eq.(2) with respect to *t*

$$\dot{\varepsilon}_{\theta\theta} = -\kappa^{n-1}\dot{\kappa}\,. \tag{23}$$

For $n = 1$, we have $\dot{\varepsilon}_{\theta\theta} = -\dot{\kappa}$, (24)

where: $\dot{\varepsilon}_{\theta\theta}$ is strain measure.

Applying $\eta \to -1$ in Eq.(14) we get

$$\kappa = \left(\frac{n}{2\mu}\right)^{\frac{1}{n}}(\sigma_{rr}-\sigma_{\theta\theta})^{\frac{1}{n}}. \tag{25}$$

Using the equations below for $\dot{\varepsilon}_{rr}$, $\dot{\varepsilon}_{\theta\theta}$, and $\dot{\varepsilon}_{zz}$ in Eq.(25), we have

$$\dot{\varepsilon}_{\theta\theta} = \left[\frac{n}{2\mu}(\sigma_{rr}-\sigma_{\theta\theta})\right]^{\frac{1}{n}-1}\left[\frac{1+\nu}{\gamma}\sigma_{ij} - \frac{\nu}{\gamma}\delta_{ij}\Theta + \alpha T\right], \text{ i.e.}$$

$$\dot{\varepsilon}_{rr} = \left[\frac{3-2C}{N(2-C)}\right]^{N-1}(\sigma_{rr}-\sigma_{\theta\theta})^{N-1}\left[T_{rr} - \left(\frac{1-C}{2-C}\right)(\sigma_{zz}+\sigma_{\theta\theta}) + \alpha T\right],$$

$$\dot{\varepsilon}_{\theta\theta}=\left[\frac{3-2C}{N(2-C)}\right]^{N-1}(\sigma_{rr}-\sigma_{\theta\theta})^{N-1}\left[\sigma_{\theta\theta}-\left(\frac{1-C}{2-C}\right)(\sigma_{rr}+\sigma_{zz})+\alpha T\right],$$

$$\dot{\varepsilon}_{zz}=\left[\frac{3-2C}{N(2-C)}\right]^{N-1}(\sigma_{rr}-\sigma_{\theta\theta})^{N-1}\left[\sigma_{zz}-\left(\frac{1-C}{2-C}\right)(\sigma_{rr}+\sigma_{\theta\theta})+\alpha T\right]=$$

$$=-\dot{\varepsilon}_0 .$$

NUMERICAL DISCUSSION

Radial and hoop stresses are represented graphically for measure $n = 1$ and 1/5, and temperature $\alpha T_0 = T_1 = 0$ and 10 against radii ratio ($r/b = R$) for cylinders made up of materials having compressibility $C = 0.3$, 0.6 and 0.9 respectively.

For linear measure, it is noticed from Fig. 2 that hoop stresses are compressible and have maximum magnitude at outer surface of cylinder at room temperature when outer pressure is greater than inner pressure. In case of nonlinear measure these stresses have maximum magnitude at inner surface of the cylinder made up of less compressible ($C =$ 0.3 and 0.6) material, while at the outer surface for cylinder of highly compressible ($C = 0.9$) material. It has been noted from Fig. 3 that hoop stresses are maximal at outer surface for homogeneous cylinder with thermal effects as compared to cylinder without thermal effects. Also, these hoop stresses have the highest value at outer surface of the cylinder with measure n =1. For nonlinear measure, hoop stresses have maximum value at inner surface. It can easily be recognized from Fig. 4 that for homogeneous circular cylinder having internal pressure higher than external pressure, the hoop stresses have maximum value at internal surface for linear measure. For nonlinear measure, the hoop stresses are higher at the inner surface for circular cylinder of highly compressible material i.e. ($C =$ 0.9) while at the outer surface for the cylinder of less compressible material i.e. ($C = 0.3$ and 0.6).

With the introduction of temperature, it is observed in Fig. 5 that for cylinder having internal pressure higher than external pressure, the hoop stresses are maximum at inner surface for linear measure while these hoop stresses have maximum value at outer surface for nonlinear measure. It is recognized from Fig. 6 that hoop stresses are compressible and maximum at the outer surface of cylinder with pressure on the outer surface. For linear measure, the magnitude of hoop stresses is maximum at outer surface for cylinder with high compressibility, $C = 0.9$, while at the inner surface for homogeneous cylinder with compressibility $C =$ 0.3 and 0.6. With the application of thermal effect, the hoop stresses show significant increase as mentioned in Fig. 7.

In Fig. 8, without thermal effects, the hoop stresses have higher value at the inner surface of cylinder with pressure at inner surface for linear measure $n =$ 1. For nonlinear measure, the hoop stresses have maximum value at the inner surface for cylinder with compressibility $C =$ 0.9, while at the outer surface for cylinder with compressibility $C =$ 0.3. Hoop stresses are approaching from tensile to compressible with temperature as mentioned in Fig. 9. The rate of change of strains is maximum at the outer surface of cylinder with measure $n =$ 1, and at the inner surface for cylinder with nonlinear measure at room temperature where pressure is higher at the outer surface than at the inner surface. The rate of change of strains decreases with temperature as can be noticed from Fig. 11. In case when pressure at the outer surface is higher, the strain rates have maximum value at the inner surface. In Fig. 12, for nonlinear measure there is a significant decrease in the rate of change of strains. The strain rates reach a maximum at the outer surface with temperature and decrease remarkably as can be noticed in Fig. 13. It is observed from Fig. 14 that in case of cylinder with measure $n =$ 1 and pressure at outer surface, the magnitude of strain rates is maximum at the outer surface and these strain rates show significant decrease with temperature. Also, these strain rates have a

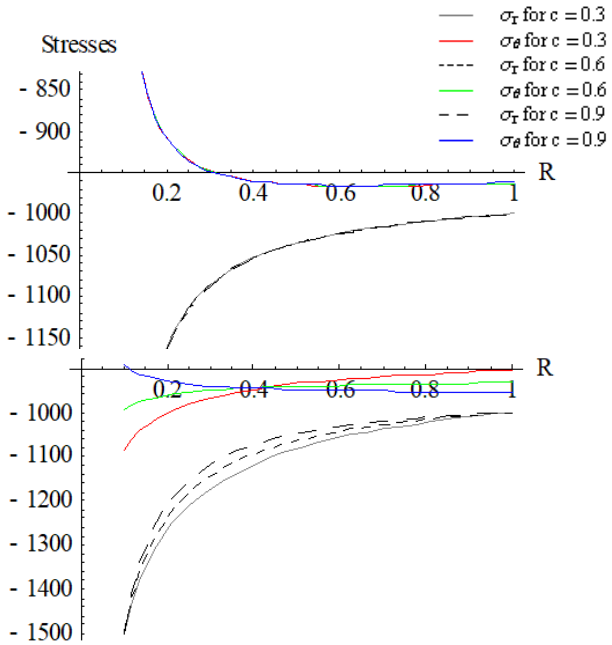

Figure 2. Variation of stresses with internal and external pressure for measure $n = 1$ and 5.

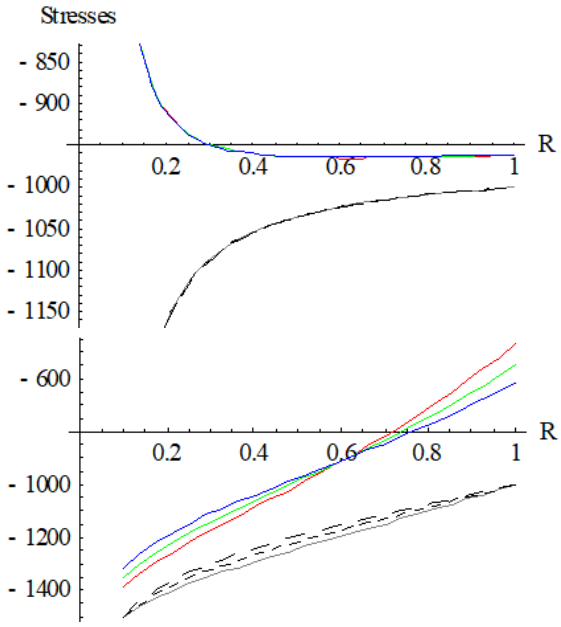

Figure 3. Variation of stresses with temperature (= 10), pressure ($P_1 = 5$ and $P_2 = 10$) for measure $n = 1$ and 5.

maximum magnitude at the outer surface for linear measure while at the inner surface for the nonlinear measure as mentioned in Fig. 15. From Fig. 16, we observe that strain rates are maximum at the inner surface for circular cylinder with pressure on the inner surface. When temperature is applied, these strain rates have a maximum at the outer surface, as can be seen in Fig. 17.

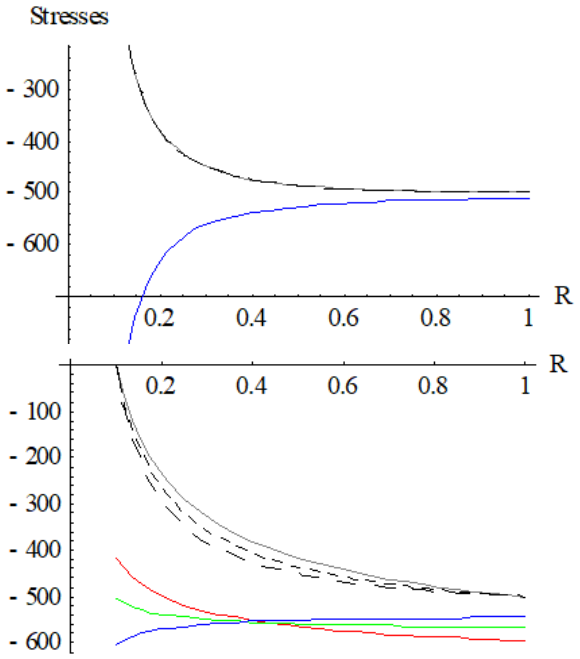

Figure 4. Variation of stresses with pressure (P_1 = 10 and P_2 = 5) for measure n = 1 and 5.

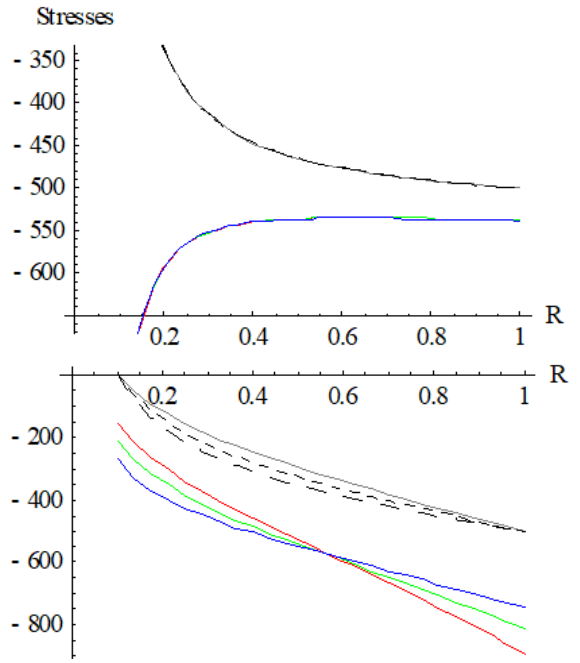

Figure 5. Variation of stresses with temperature (= 10), pressure (P_1 = 10 and P_2 = 5) for measure n = 1 and 5.

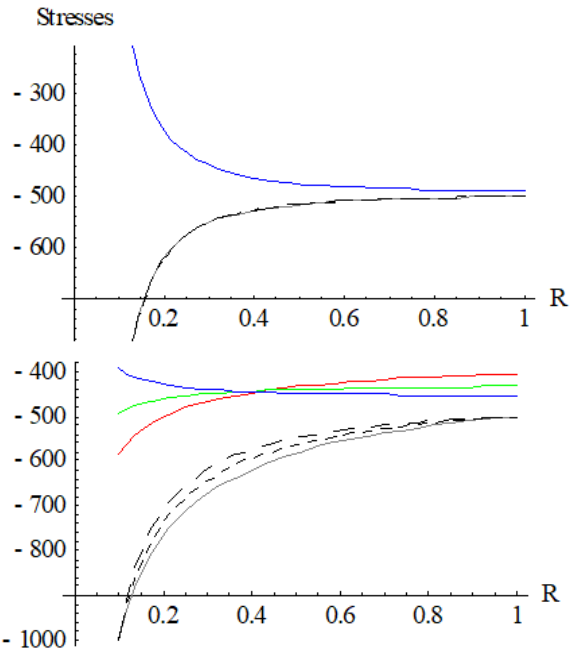

Figure 6. Variation of stresses with pressure (P_1 = 0 and P_2 = 5) for measure n = 1 and 5.

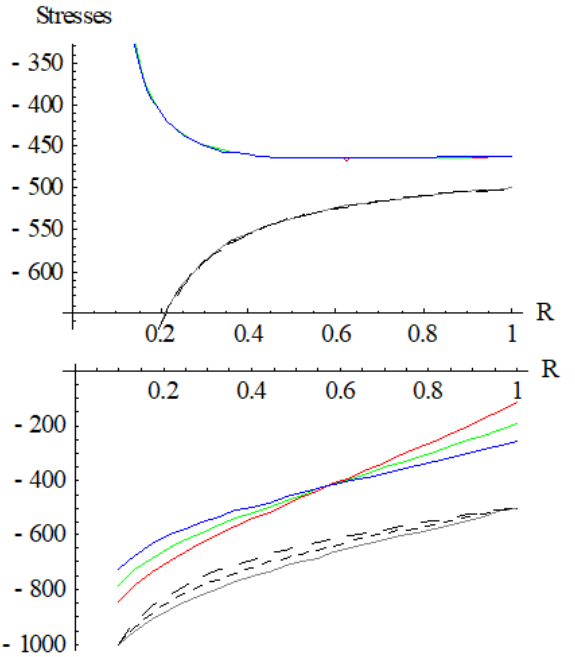

Figure 7. Variation of stresses with temperature (= 10), pressure (P_1 = 0 and P_2 = 5) for measure n = 1 and 5.

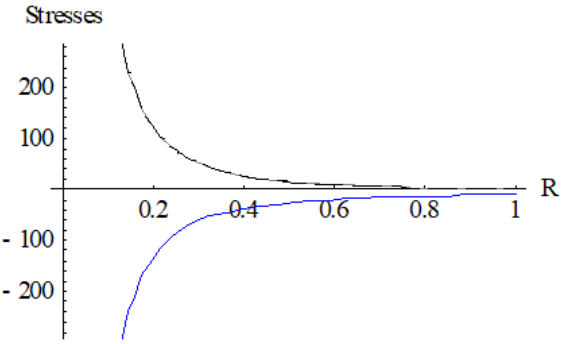

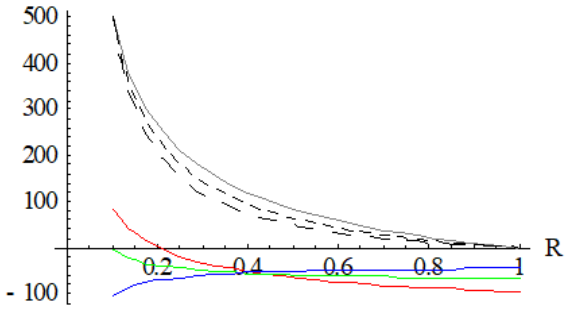

Figure 8. Variation of stresses with pressure ($P_1 = 5$ and $P_2 = 0$) for measure $n = 1$ and 5.

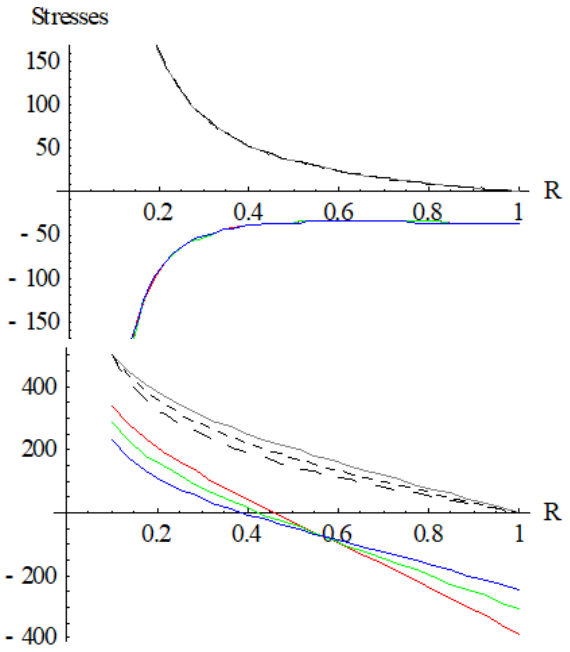

Figure 9. Variation of stresses with temperature (= 10), pressure ($P_1 = 5$ and $P_2 = 0$) for measure $n = 1$ and 5.

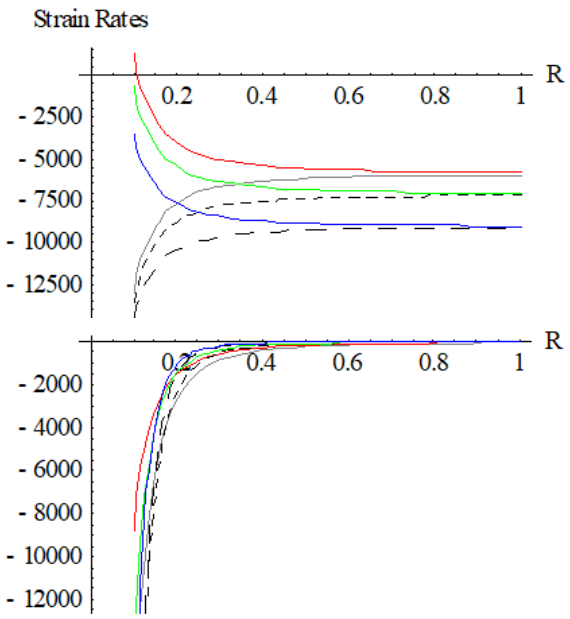

Figure 10. Variation of strains with pressure ($P_1 = 5$ and $P_2 = 10$) for measure $n = 1$ and 5.

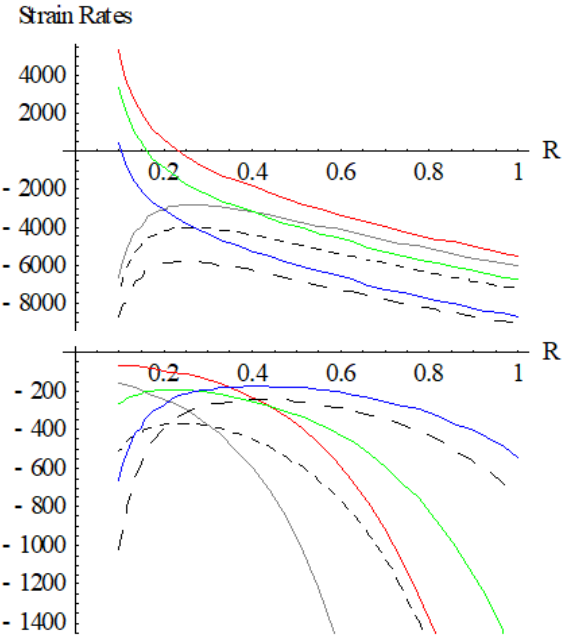

Figure 11. Variation of strains with temperature (= 10), pressure ($P_1 = 5$ and $P_2 = 10$) for measure $n = 1$ and 5.

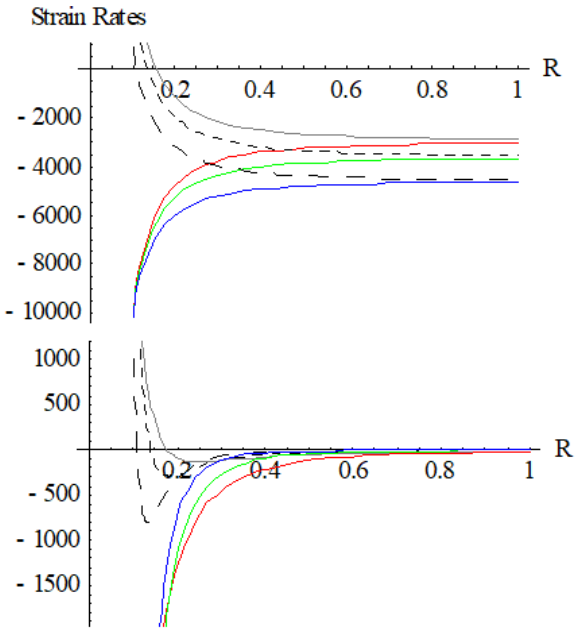

Figure 12. Variation of strains with pressure ($P_1 = 10$ and $P_2 = 5$) for measure $n = 1$ and 5.

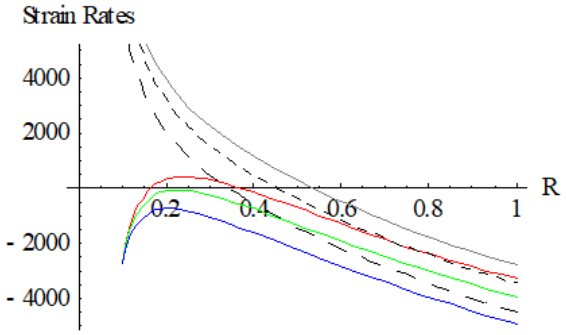

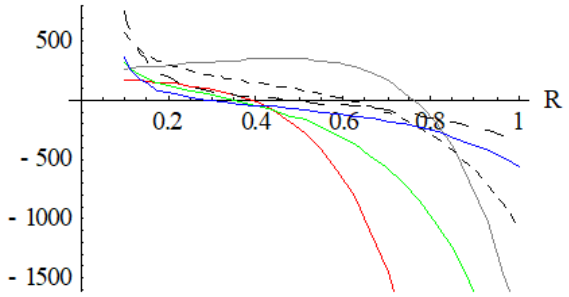

Figure 13. Variation of strains with temperature (= 10), pressure (P_1 = 10 and P_2 = 5) for measure n = 1 and 5.

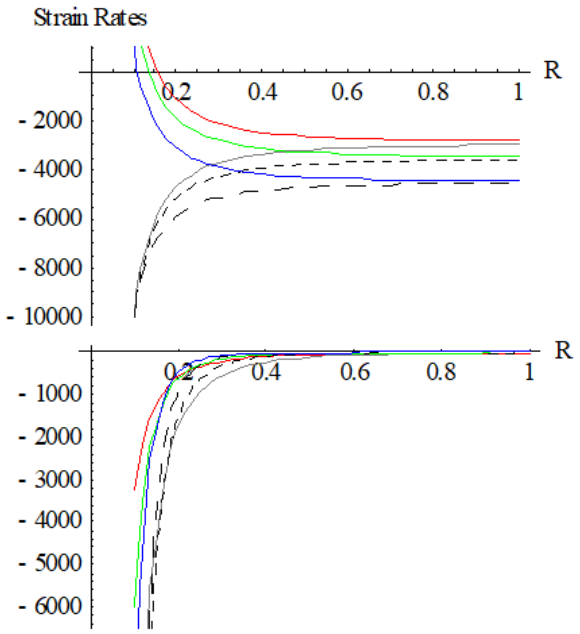

Figure 14. Variation of strains with pressure (P_1 = 0 and P_2 = 5) for measure n = 1 and 5.

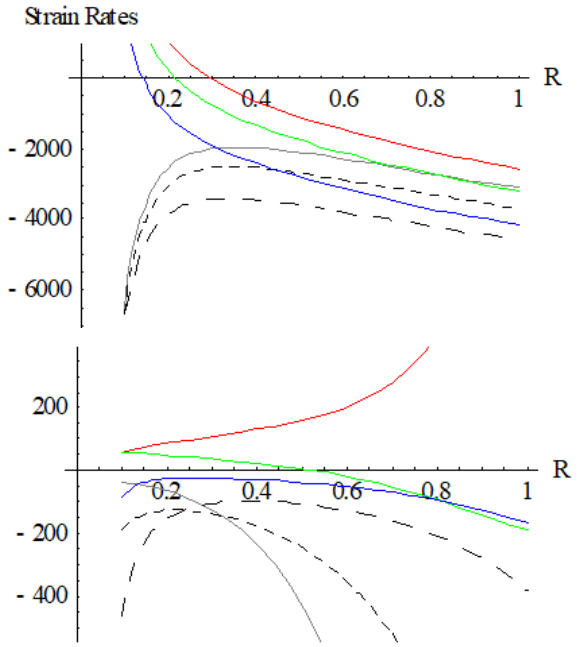

Figure 15. Variation of strains with temperature (= 10), pressure (P_1 = 0 and P_2 = 5) for measure n = 1 and 5.

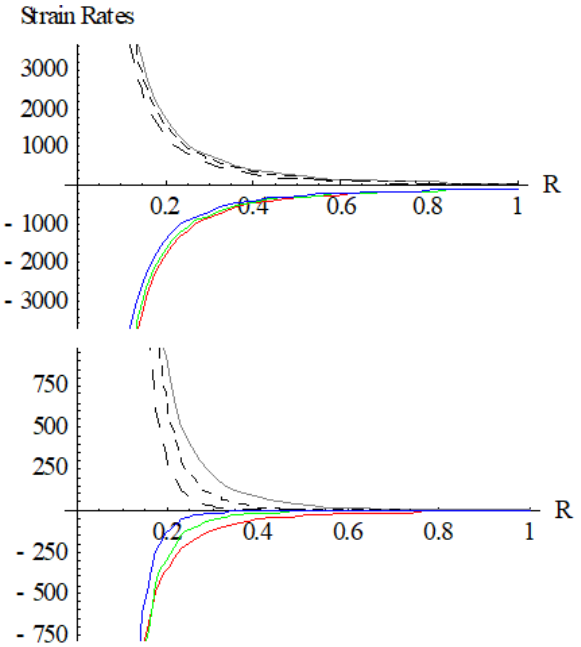

Figure 16. Variation of strains with pressure (P_1 = 5 and P_2 = 0) for measure n = 1 and 5.

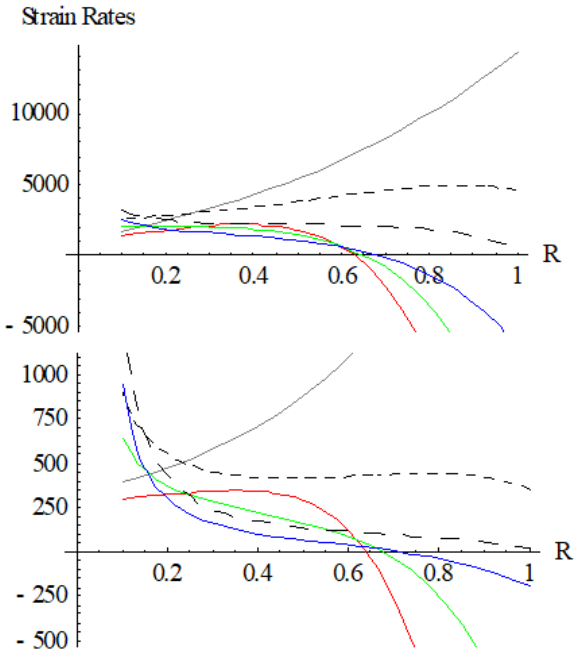

Figure 17. Variation of strains with temperature (= 10), pressure (P_1 = 5 and P_2 = 0) for measure n = 1 and 5.

REFERENCES

1. Altenbach, H., Skrzypek, J.J. (1999), Creep and Damage in Materials and Structures, Springer Verlag, Berlin.
2. Kraus, H. (1980), Creep Analysis, Wiley, New York, Toronto.
3. Rimrott, F.P.J., Luke, J.R. (1961), *Large strain creep of rotating cylinders*, ZAMM, 42(12): 485-500.
4. Bhatnagar, N.S., Kulkarni, P.S., Arya, V.K. (1984), *Creep analysis of an internally pressurized orthotropic rotating cylinder*, Nuclear Eng. and Design, 83(3): 379-388.
5. Kashkoli, M.D., Nejad, M.Z. (2014), *Effect of heat flux on creep stresses of thick-walled cylindrical pressure vessels*, J Appl. Res. and Techn., 12(5): 85-97.

6. Loghman, A., Ghorbanpour, A., Aleayoub, S.M. (2011), *Time-dependent creep stress redistribution analysis of thick-walled functionally graded spheres*, Mech. of Time-Dependent Mat., 15(4): 353-365.
7. You, L.H., Ou, H., Zheng, Z.Y. (2007), *Creep deformations and stresses in thick-walled cylindrical vessels of functionally graded materials subjected to internal pressure*, Compos. Struc., 78(2): 285-291.
8. Singh, T., Gupta, V.K. (2011), *Effect of anisotropy on steady state creep in functionally graded cylinder*, Compos. Struc., 93(2): 747-758.
9. Seth, B.R. (1974), *Creep transition in rotating cylinders*, J Math. and Phys. Sci., 8(1): 1-5.
10. Seth, B.R. (1966), *Measure concept in mechanics*, Int. J Non-linear Mech., 1(1): 35-40.
11. Sharma, S. (2009), *Thermo creep transition in non-homogeneous thick-walled rotating cylinders*, Defence Science J, 59(1): 30-36.
12. Sharma, S., Sahni, M., Kumar, R. (2009), *Elastic-plastic transition of transversely isotropic thick-walled rotating cylinder under internal pressure*, Defence Science J, 59(3): 60-264.
13. Aggarwal, A.K., Sharma, R., Sharma, S. (2013), *Safety analysis using Lebesgue strain measure of thick-walled cylinder for functionally graded material under internal and external pressure*, The Sci. World J, doi.org/10.1155/2013/676 190:1-10.
14. Aggarwal, A.K., Sharma, R., Sharma, S. (2014), *Collapse pressure analysis of transversely isotropic thick-walled cylinder using Lebesgue strain measure and transition theory*, The Sci. World J, dx.doi.org/10.1155/2014/240954: 1-10.
15. Sharma S., Yadav, S. (2013), *Thermo elastic-plastic analysis of rotating functionally graded stainless steel composite cylinder under internal and external pressure using finite difference method*, Advan. in Mat. Sci. and Eng., doi.org/10.1155/2013/810508: 1-10.
16. Sharma, S., Yadav, S., Sharma, R. (2017), *Thermal creep analysis of functionally graded thick-walled cylinder subjected to torsion and internal and external pressure*, J Solid Mech., 9(2): 302-318.
17. Sharma, S., Panchal, R. (2017), *Thermal creep deformation in pressurized thick-walled functionally graded rotating spherical shell*, Int. J Pure and Appl. Math., 114(3): 435-444.
18. Sharma, S. (2017), *Stress analysis of elastic-plastic thick-walled cylindrical pressure vessels subjected to temperature*, Struc. Integ. and Life, 17(2):105-112.
19. Sharma, S. (2017), *Creep transition in bending of functionally graded transversely isotropic rectangular plates*, Struc. Integ. and Life, 17(3): 187-192.

ESIS ACTIVITIES and

CALENDAR OF CONFERENCES, TC MEETINGS, and WORKSHOPS

June 4-6, 2018	IGF Workshop Fracture and Structural Integrity: ten years of 'Frattura ed integrità Strutturale'	Cassino, Italy	link
June 17-20, 2018	1st International Conference on Theoretical, Applied and Experimental Mechanics (ICTAEM 1)	Paphos, Cyprus	https://www.ictaem.org/
July 1-5, 2018	18th International Conference on Experimental Mechanics (ICEM 2018)	Brussels, Belgium	http://www.icem18.org/
July 2-6, 2018	10th European Solid Mechanics Conference (ESMC 2018)	Bologna, Italy	http://www.esmc2018.org
July 5-6, 2018	2nd International Conference on Materials Design and Applications	Porto, Portugal	https://web.fe.up.pt/~mda2018/
July 8-11, 2018	8th Internat. Conference on Engineering Failure Analysis (ICEFA VIII)	Budapest, Hungary	link
August 25-26, 2018	ESIS Summer School in the scope of ECF22	Belgrade, Serbia	link
August 26-31, 2018	22nd European Conference of Fracture (ECF22)	Belgrade, Serbia	http://www.ecf22.rs
September 19-21, 2018	CP 2018- 6th International Conference on 'Crack Paths'	Verona, Italy	http://www.cp2018.unipr.it/
June 24-26, 2019	12th International Conference on Multiaxial Fatigue and Fracture (ICMFF12)	Bordeaux, France	link
March 30 - April 3, 2020	VAL4, 4th International Conference on Material and Component Performance under Variable Amplitude Loading	Darmstad, Germany	First Announcement